

# Quantum superresolution in fluorescence microscopy

O. Schwartz,<sup>1</sup> J.M. Levitt,<sup>1</sup> R. Tenne,<sup>1</sup> S. Itzhakov,<sup>1</sup> Z. Deutsch,<sup>1</sup> and D. Oron<sup>1</sup>

<sup>1</sup>*Department of Physics of Complex Systems, Weizmann Institute of Science, Rehovot, Israel*

The optical diffraction limit, formulated by Abbe 150 years ago, decades before the dawn of quantum mechanics, imposes a bound on imaging resolution in classical optics. Over the last twenty years, many theoretical schemes have been presented for overcoming the diffraction barrier in optical imaging using quantum properties of light. An experimental realization of sub-diffraction limited quantum imaging has, however, remained elusive. Here, we take advantage of non-classical light naturally produced in fluorescence microscopy due to photon antibunching, a fundamentally quantum phenomenon ensuring that fluorophores emit photons one at a time. Using a photon counting digital camera, we detect antibunching-induced second and third order intensity correlations and perform sub-diffraction limited quantum imaging in a standard wide-field fluorescence microscope.

During the last decade, quantum-based strategies have opened new possibilities in information processing, metrology, and imaging. One of the most ambitious endeavors in this field is overcoming the diffraction barrier in optical imaging by employing quantum states of light.

The diffraction limit restricts the resolution of optical microscopes to approximately half the wavelength of light. Abbe's description of the imaging system[1] is based on the laws of classical linear optics, applied to stationary objects. Correspondingly, there are three loopholes in the argument, concerning the linearity, stationarity, and classicality assumptions. In the last two decades, super-resolution imaging methods were developed based on nonlinear optical effects such as stimulated emission[2], optical shelving[3] and fluorescence saturation[4, 5]. More recently, sub-diffraction limited imaging was achieved by another class of microscopy methods, making use of non-stationary emission of fluorescent markers caused either by photo-switching[6–8], or by intrinsic brightness fluctuations [9, 10].

The remaining loophole for overcoming the diffraction barrier, resorting to quantum optics, has received a lot of attention in the recent years. It has been shown that high order quantum interference patterns arising in quantum optics can yield spatial distribution of correlations much tighter than classically allowed. Such fringes have been observed using coincidence detection in various settings[11–13]. It seems tempting to use these sharp spatial features to image sub-wavelength details of microscopic objects. Several quantum superresolution schemes have been proposed, utilizing multi-mode squeezed light[14], an arrangement of single photon emitters[15], or generalized quantum states of light[16, 17]. At the same time, although quantum optical methods have enabled image entanglement[18] and sub-shot noise imaging[19], as well as quantum optical coherence tomography with improved depth resolution[20], sub-diffraction limited quantum imaging has not yet been experimentally demonstrated.

The common element of most proposed quantum superresolution schemes is illuminating an absorptive sample with a nonclassical state of light. An alternative ap-

proach, proposed theoretically by Hell et al.[21], relies on non-classical properties of light emitted by the sample itself, while using regular laser light for illumination. It was shown in this work that a hypothetical quantum emitter producing photons only in pairs (or groups) can be imaged using coincidence detection with a resolution increase similar to that attainable in two-photon (multi-photon) microscopy. Unfortunately, the technique has not been taken up experimentally since no suitable multi-photon emitting fluorophore has ever been introduced.

Here, we extend the idea of multi-photon detection put forward by Hell et al. by utilizing fluorophores in which emission of more than one photon is suppressed. This phenomenon, known as photon antibunching[22], is observed in most common fluorophores, such as organic dyes[23, 24] or quantum dots[25, 26], even under ambient conditions. The necessary quantum emitters are thus widely used in fluorescence microscopy, a ubiquitous life science imaging tool. Due to photon antibunching, in every point of the image plane of a fluorescence microscope photon statistics is sub-Poissonian[27], i.e. the number of simultaneous multi-photon detection events is smaller in every order than it is for classical light. Quantifying the missing N-photon coincidence events gives a signal equivalent to N-photon detection signal, narrowing the effective point spread function by a factor of  $\sqrt{N}$ [28]. In this work, we detect photon statistics in the image plane of a wide-field fluorescence microscope, determine the spatial distribution of missing two- and three-photon coincidence events, and reconstruct second and third order superresolved images.

Our measurement scheme relies on detecting fluorescence intensity correlations. When a perfectly antibunched quantum emitter is imaged onto a detector array, the single photon it emits following excitation can arrive to only one of the detectors. While classically the detector readings would be uncorrelated, antibunching thus creates negative correlations between them. Importantly, contributions to connected correlation functions from individual fluorophores are additive, and can therefore be utilized as a local measure of the emitter density, thus directly providing superresolved images of the fluo-

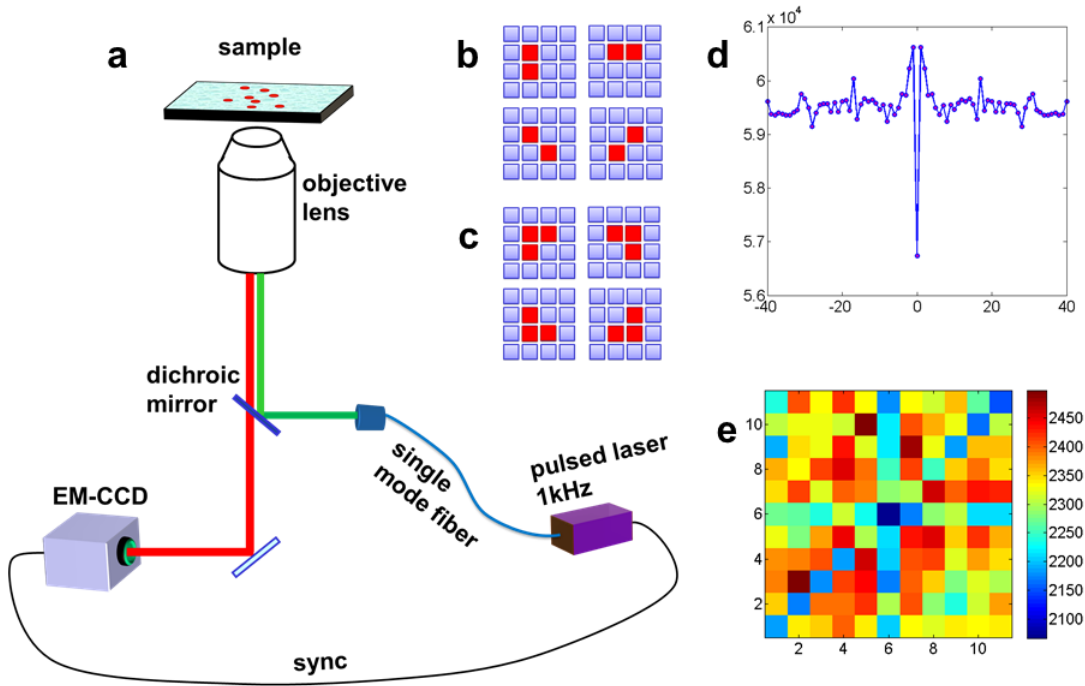


FIG. 1. Detecting nonclassical correlations in fluorescence microscopy: (a) A schematic of experimental setup used for correlation imaging, (b) pixel configurations used for 2-point correlation detection (c) pixel configurations used for 3-point correlation detection, (d) second order autocorrelation of a signal from a single QD featuring an antibunching dip, (e) two-dimensional plot representing third order autocorrelation from the same QD

rophore spatial distribution.

Experimental observation of nonclassical intensity correlations was carried out using a regular wide-field epi-fluorescence microscope shown schematically in Fig. 1a (see Supporting Information for additional details). For the proof of principle demonstration of antibunching imaging, we used test samples consisting of CdSe/CdS/ZnS colloidal quantum dots (QDs), commonly used as labels in fluorescence microscopy[29], deposited on a glass substrate. The main emission peak of the QDs was at 610 nm, and their fluorescence lifetime was 32ns (see Supporting Information for further details). Such QDs demonstrate strong photon antibunching due to

Auger interaction between excitons, inhibiting emission of more than one photon following photoexcitation[25]. These QDs were recently shown to exhibit nearly absolute photostability under similar conditions[30].

To detect photon statistics simultaneously in the entire field of view, we used an electron multiplying charge-coupled device (EMCCD) in the photon counting mode as a fluorescence detector. The fluorophores were excited with 300 ps laser pulses at 532 nm, with pulse energy close to saturation. Following emitter relaxation, the image was read out and stored in a computer. The excitation pulse/image readout sequence was repeated at a rate of 1kHz. The pixel readings were thresholded to

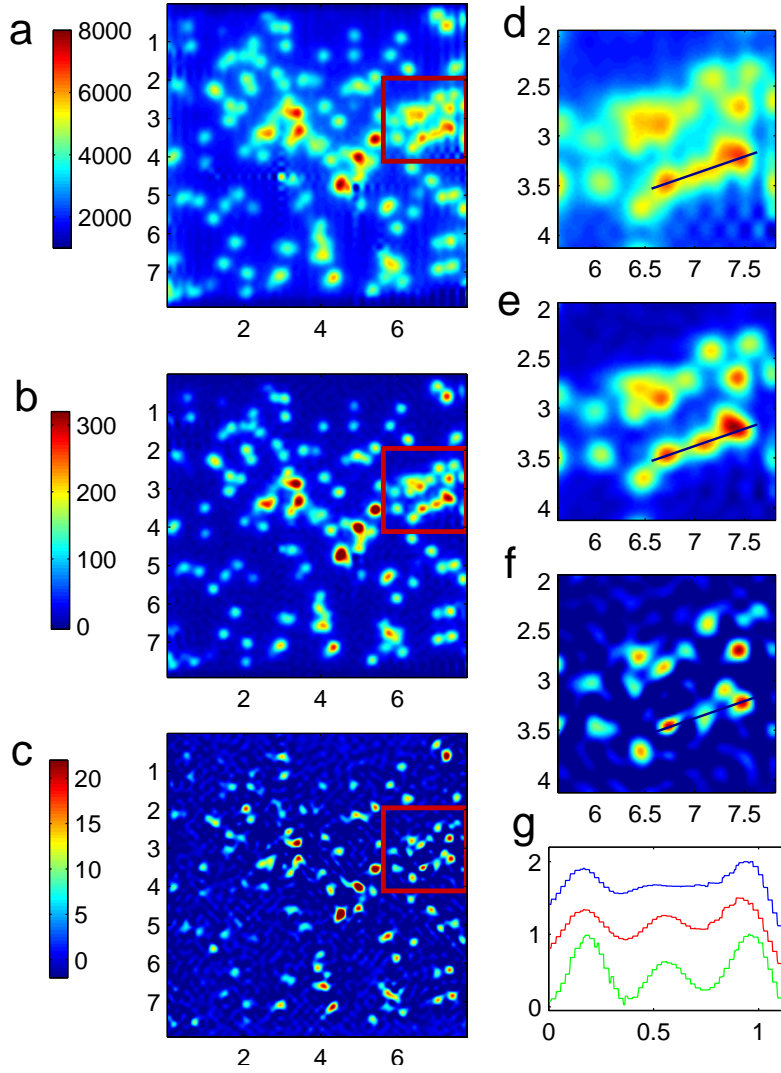


FIG. 2. Fluorescence antibunching imaging: panels a-c show regular fluorescence image, second and third order antibunching images. Panels d-f show magnified views of the area indicated by the red square in the images a-c. The graph presented in panel g shows a cut of the magnified images along the line indicated in panels d-f. The blue line corresponds to regular fluorescence image, the red and green lines represent the second and third order antibunching imaging, respectively. The lines are vertically shifted for visibility. All coordinates are given in microns.

produce maps of photon detection events, neglecting the probability of detecting more than one photon per pixel in the same excitation cycle.

Pulsed excitation in combination with image readout after every exposure allowed us to detect correlation functions exhibiting the characteristic antibunching dip at zero delay simultaneously for multiple emitters in the field of view. A typical signal autocorrelation curve from a single emitter is shown in Fig. 1d. The autocorrelation curve represents the sum of cross-correlations of all pixel pairs within a small region corresponding to the image of the fluorophore. The horizontal axis shows the discrete time delay in units of the interval between pulses (1 ms). Furthermore, we were able to detect the an-

tibunching features in the three-point correlation function, quantifying the relations between signal values at three different points in time. A two-dimensional plot of a typical three-point correlation function, depending on two discrete delay times  $\tau_1$  and  $\tau_2$ , is shown in Fig. 1e. The plot features depressed lines at  $\tau_1 = 0$ , at  $\tau_2 = 0$  and at  $\tau_1 = \tau_2$ , which represent the lack of two-photon coincidence events. The central datapoint of this plot, at  $\tau_1 = \tau_2 = 0$ , which is depressed even further, represents the missing three-photon coincidence events. The dips in the temporal autocorrelation functions represent the non-classical signal that we proceed to utilize to produce superresolved images.

To quantify the second order quantum correlations at

every point in the image plane with sub-diffraction limited resolution, we computed the cross-correlations between pairs of neighboring pixels in configurations shown in Fig. 1b. The resulting four correlation maps were Fourier-interpolated and summed. Similarly, the third order quantum images were obtained by computing the connected third order cross-correlation for pixel configurations shown in Fig. 1c. The details of the data processing are described in the Supporting Information.

A typical superresolved image set is shown in Fig. 2. A regular fluorescence image and the second and third order antibunching images of the same area, presented in panels (a-c) of Fig. 2, demonstrate consecutive improvement of resolution. The magnified view of a small region (panels d-f of Fig. 2) illustrates the initially unresolved features of QD distribution revealed by antibunching imaging. Enhanced resolution is also evident in the line scan plotted in Fig. 2(g). Quantitatively, the resolution improves from the diffraction-limited 280 nm to 220 nm in the second order and 180 nm in the third order, corresponding to a resolution enhancement by a factor of 1.55, close to the theoretically expected improvement of  $\sqrt{3}$ .

In addition to improving the transverse resolution, antibunching imaging has an optical sectioning capability similar to that demonstrated by multi-photon excitation microscopy. This is illustrated by the out-of-focus images of a QD presented in Fig. 3. A comparison of the regular fluorescent images of Fig. 3(a-c) with the corresponding second order antibunching images shown in Fig. 3(d-f) demonstrates that the antibunching signal decreases faster with defocusing than regular fluorescence. While the regular fluorescence signal is blurred by defocusing, in transparent medium its integral remains unchanged, leading to out-of-focus background in wide-field microscopy. In contrast, the second order antibunching signal fades away quadratically with defocusing, leading to discrimination of the out-of-focus signal. Fig. 3g shows the integral signal variation as a function of defocusing for regular fluorescence imaging and for the second order antibunching signal.

The superresolved imaging method presented here is based on a genuine quantum property of light arising in non-resonant fluorescence. The antibunching signal used to produce superresolved images above quantifies the dip at zero delay in the intensity correlation functions, which has no analog in classical optics. Equivalently, it can be thought of as originating from sub-Poissonian photon statistics of antibunched light, which cannot be described classically either[31].

The antibunching based superresolution imaging method presented here is closely related to Superresolution Optical Fluctuation Imaging (SOFI) [10]. In both approaches, intensity correlations are detected in the image plane of a fluorescence microscope and used to produce superresolved images. The main difference between

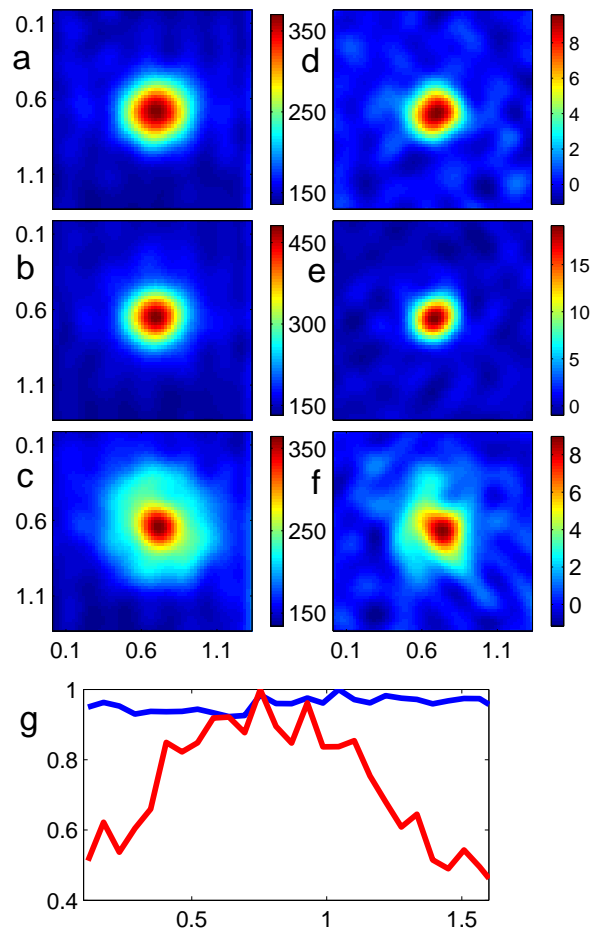


FIG. 3. Regular fluorescence and second order antibunching imaging dependence on defocusing. Panels a-c show the images of a QD with the imaging system focused 360nm below the object plane(a), right on it(b), and 360 nm above (c). Panels d-f show the corresponding second order antibunching images. Panel g shows the total signal, integrated over the field of view, as a function of defocusing. The blue line represents regular fluorescence, the red line corresponds to second order antibunching imaging. While integrated fluorescence signal is almost constant as a function of depth, the integrated antibunching signal decays quickly with defocusing. All coordinates are given in microns.

the two approaches is the source of the signal fluctuations recovered via correlations: fluorophore brightness fluctuations leading to super-Poissonian photon statistics in SOFI, and antibunched emission resulting in sub-Poissonian statistics in case of antibunching microscopy. Correspondingly, the SOFI signal is highly dependent on the character of emission fluctuations exhibited by the fluorophores, which varies widely from one species to another[32], while in antibunching imaging the statistical properties of signal giving rise to the superresolved images are universal, arising from steady emission of fluorophores with no fluctuations other than antibunching-

modified shot noise.

Performance of antibunching imaging is limited at present by the parameters of the EMCCD used for photon detection. The data acquisition rate was limited by the image readout speed, while a major contribution to noise came from the false photon counts. The rapid progress of the photon detector technologies in the recent years gives hope that fast and low-noise detectors will become available in the near future, which will dramatically improve the practical prospects of antibunching imaging.

Although in our setup the sample is uniformly illuminated, antibunching imaging can be synergetically combined with patterned excitation microscopy[4]. Indeed, correlation signal of order  $N$  is proportional to the  $N$ -th power of the excitation power (assuming non-saturated fluorophores), which, in combination with correlation detection, can produce images with even higher resolution.

In summary, we have demonstrated that non-classical statistical properties of the photon stream used to create images in fluorescence microscopy can be harnessed for sub-diffraction-limited quantum imaging. The experiment was carried out at room temperature with regular QD fluorophores, suggesting that this approach might develop into an attractive alternative to existing super-resolution microscopy methods in life science imaging.

#### ACKNOWLEDGEMENTS

- 
- [1] Ernst Abbe. Beiträge zur theorie des mikroskops und der mikroskopischen wahrnehmung. *Arch. Mikrosk. Anat.*, 9:413, 1873.
- [2] S.W. Hell and J. Wichmann. Breaking the diffraction resolution limit by stimulated emission: stimulated-emission-depletion fluorescence microscopy. *Opt. Lett.*, 19(11):780–782, 1994.
- [3] Marcus Dyba Stefan W. Hell and Stefan Jakobs. Concepts for nanoscale resolution in fluorescence microscopy. *Current Opinion in Neurobiology*, 14:599–609, 2004.
- [4] M. G. L. Gustafsson. Nonlinear structured-illumination microscopy: Wide-field fluorescence imaging with theoretically unlimited resolution. *Proc. Nat. Acad. Sci.*, 102:13081–13086, September 2005.
- [5] Katsumasa Fujita, Minoru Kobayashi, Shogo Kawano, Masahito Yamanaka, and Satoshi Kawata. High-resolution confocal microscopy by saturated excitation of fluorescence. *Phys. Rev. Lett.*, 99(22):228105, 2007.
- [6] E. Betzig, G.H. Patterson, R. Sougrat, O.W. Lindwasser, S. Olenych, J.S. Bonifacino, M.W. Davidson, J. Lippincott-Schwartz, and H.F. Hess. Imaging intracellular fluorescent proteins at nanometer resolution. *Science*, 313(5793):1642, 2006.
- [7] S.T. Hess, T.P.K. Girirajan, and M.D. Mason. Ultra-high resolution imaging by fluorescence photoactivation localization microscopy. *Biophys. J.*, 91(11):4258–4272, 2006.
- [8] Mark Bates Michael J. Rust and Xiaowei Zhuang. Sub-diffraction-limit imaging by stochastic optical reconstruction microscopy (storm). *Nature Methods*, 3:793–796, 2006.
- [9] K. Lidke, B. Rieger, T. Jovin, and R. Heintzmann. Super-resolution by localization of quantum dots using blinking statistics. *Opt. Express*, 13(18):7052–7062, 2005.
- [10] T. Dertinger, R. Colyer, G. Iyer, S. Weiss, and J. Enderlein. Fast, background-free, 3D super-resolution optical fluctuation imaging (SOFI). *Proc. Nat. Acad. Sci.*, 106(52):22287, 2009.
- [11] P. Walther, J.W. Pan, M. Aspelmeyer, R. Ursin, S. Gasparoni, and A. Zeilinger. De Broglie wavelength of a non-local four-photon state. *Nature*, 429(6988):158–161, 2004.
- [12] I. Afek, O. Ambar, and Y. Silberberg. High-NOON States by Mixing Quantum and Classical Light. *Science*, 328(5980):879, 2010.
- [13] Ryan S. Bennink, Sean J. Bentley, Robert W. Boyd, and John C. Howell. Quantum and classical coincidence imaging. *Phys. Rev. Lett.*, 92:033601, Jan 2004. H. Shin, K.W.C. Chan, H.J. Chang, and R.W. Boyd. Quantum spatial superresolution by optical centroid measurements. *Physical Review Letters*, 107(8):83603, 2011.
- [14] Mikhail I. Kolobov and Claude Fabre. Quantum limits on optical resolution. *Phys. Rev. Lett.*, 85:3789–3792, Oct 2000.
- [15] C. Thiel, T. Bastin, J. von Zanthier, and GS Agarwal. Sub-rayleigh quantum imaging using single-photon sources. *Physical Review A*, 80(1):13820, 2009. C. Thiel, T. Bastin, J. Martin, E. Solano, J. Von Zanthier, and GS Agarwal. Quantum imaging with incoherent photons. *Phys. Rev. Lett.*, 99(13):133603, 2007.
- [16] B.E.A. Saleh, M.C. Teich, and A.V. Sergienko. Wolf equations for two-photon light. *Physical review letters*, 94(22):223601, 2005.
- [17] V. Giovannetti, S. Lloyd, L. Maccone, and J.H. Shapiro. Sub-rayleigh-diffraction-bound quantum imaging. *Physical Review A*, 79(1):013827, 2009. Fabrizio Guerrieri, Lorenzo Maccone, Franco N. C. Wong, Jeffrey H. Shapiro, Simone Tisa, and Franco Zappa. Sub-rayleigh imaging via  $n$ -photon detection. *Phys. Rev. Lett.*, 105(16):163602, Oct 2010.
- [18] Vincent Boyer, Alberto M. Marino, Raphael C. Pooser, and Paul D. Lett. Entangled images from four-wave mixing. *Science*, 321(5888):544–547, 2008.
- [19] G. Brida, M. Genovese, and I.R. Berchera. Experimental realization of sub-shot-noise quantum imaging. *Nature Photonics*, 4(4):227–230, 2010.
- [20] Maged B. Nasr, Bahaa E. A. Saleh, Alexander V. Sergienko, and Malvin C. Teich. Demonstration of dispersion-canceled quantum-optical coherence tomography. *Phys. Rev. Lett.*, 91:083601, Aug 2003.
- [21] S.W. Hell, J. Soukka, and P.E. Hänninen. Two-and multiphoton detection as an imaging mode and means of increasing the resolution in far-field light microscopy: A study based on photon-optics. *Bioimaging*, 3(2):64–69, 1995.
- [22] H. J. Kimble, M. Dagenais, and L. Mandel. Photon antibunching in resonance fluorescence. *Phys. Rev. Lett.*, 39(11):691–695, 1977.

- [23] T. Basché, WE Moerner, M. Orrit, and H. Talon. Photon antibunching in the fluorescence of a single dye molecule trapped in a solid. *Physical review letters*, 69(10):1516–1519, 1992.
- [24] W.P. Ambrose, P.M. Goodwin, J. Enderlein, D.J. Semin, J.C. Martin, and R.A. Keller. Fluorescence photon antibunching from single molecules on a surface. *Chem. Phys. Lett.*, 269(3-4):365–370, 1997.
- [25] B. Lounis, HA Bechtel, D. Gerion, P. Alivisatos, and WE Moerner. Photon antibunching in single CdSe/ZnS quantum dot fluorescence. *Chem. Phys. Lett.*, 329(5-6):399–404, 2000.
- [26] P. Michler, A. Imamoglu, MD Mason, PJ Carson, GF Strouse, and SK Buratto. Quantum correlation among photons from a single quantum dot at room temperature. *Nature*, 406:968–970, 2000.
- [27] L. Mandel. Sub-Poissonian photon statistics in resonance fluorescence. *Opt. Lett.*, 4(7):205–207, 1979.
- [28] O. Schwartz and D. Oron. Improved resolution in fluorescence microscopy using quantum correlations. *Physical Review A*, 85(3):33812, 2012.
- [29] X. Michalet, FF Pinaud, LA Bentolila, JM Tsay, S. Doose, JJ Li, G. Sundaresan, AM Wu, SS Gambhir, and S. Weiss. Quantum dots for live cells, in vivo imaging, and diagnostics. *Science*, 307(5709):538–544, 2005.
- [30] O. Schwartz, R. Tenne, J.M. Levitt, Z. Deutsch, S. Itzhakov, and D. Oron. Colloidal quantum dots as saturable fluorophores. *ACS nano*, 2012.
- [31] D. F. Walls and P. Zoller. Reduced quantum fluctuations in resonance fluorescence. *Phys. Rev. Lett.*, 47(10):709–711, Sep 1981.
- [32] F. Cichos, C. von Borczyskowski, and M. Orrit. Power-law intermittency of single emitters. *Current Opinion in Colloid & Interface Science*, 12(6):272 – 284, 2007.